Table 3 Diplotypes and allele frequencies of *CES1A* genes in Caucasians, African–Americans, and Japanese

Group	*CES1A1* genotype	*CES1A3* or *CES1A2* genotype	Number of participants		
			Caucasians	African–Americans	Japanese
I	W/W	1A3/1A3	50	66	31
II	W/W	1A3/1A2	20	8	26
III	W/W	1A2/1A2	1	0	5
IV	W/V	1A3/1A3	22	27	12
V	W/V	1A3/1A2	8	2	21
VI	W/V	1A2/1A2	0	0	3
VII	V/V	1A3/1A3	3	3	6
VIII	V/V	1A3/1A2	0	1	2
IX	V/V	1A2/1A2	0	0	1
Total			104	107	107
Genotype			Frequency (%)		
CES1A1					
CES1A1 wild type			82.7	82.7	74.8
CES1A1 variant			17.3	17.3	25.2
CES1A3 or *CES1A2*					
CES1A3			85.6	94.9	68.7
CES1A2			14.4	5.1	31.3

CES, *carboxylesterase*; V, variant; W, wild type.

Table 4 CES1A1 and CES1A2 mRNA levels in human livers

Group	Number of samples	*CES1A1* genotype	*CES1A3* or *CES1A2* genotype	CES1A1/GAPDH mRNA (copy/0.1 μg)		CES1A2/GAPDH mRNA (copy/0.1 μg)	
				Mean ± SD	Range	Mean ± SD	Range
I	17	W/W	1A3/1A3	15.7 ± 13.7	(2.1–52.9)	ND	
II	17	W/W	1A3/1A2	22.3 ± 16.0	(4.2–61.7)	0.3 ± 0.3	(0.0–0.8)
III	3	W/W	1A2/1A2	25.8 ± 18.2	(10.0–45.7)	0.5 ± 0.5	(0.0–1.2)
IV	5	W/V	1A3/1A3	16.0 ± 12.1	(2.3–26.8)	8.2 ± 7.0	(0.0–15.0)
V	9	W/V	1A3/1A2	7.9 ± 7.8	(1.7–27.9)	4.8 ± 4.8	(0.7–16.9)
VI	1	W/V	1A2/1A2	23.8		13.3	
VII	1	V/V	1A3/1A2	ND		5.3	
VIII	2	V/V	1A2/1A2	ND		5.6	(2.5–8.6)

CES, *carboxylesterase*; GAPDH, glyceraldehyde-3-phosphate dehydrogenase; ND, not detected; V, variant; W, wild type.

cell carcinoma cell line KYSE. In addition, Hosokawa *et al.* [15] recently reported that transcriptional factors Sp 1 and C/EBP could bind to the *CES1A1* promoter region, but not to the *CES1A2* promoter region by a luciferase assay using human hepatoma cell line FLC7 and Drosophila SL2 as well as a gel shift mobility assay. These results suggest that subtle differences in the sequences at the 5′-flanking region between *CES1A1* and *CES1A2* affect the transcriptional activity. Supporting their report, in our human liver samples, the levels of CES1A2 mRNA transcribed from the *CES1A2* gene were substantially lower than those transcribed from the *CES1A1* variant (Table 4). CES1A3 mRNA was not detected in the human liver samples (data not shown). Thus, it is conceivable that the *CES1A3* promoter (identical with the *CES1A2* promoter) might be hardly active in human livers. CES1A3 complementary DNA was originally cloned (named PCE-3) from human placenta [9]. Therefore, in some extrahepatic tissues such as placenta, small intestine, colon, kidney, and lung, the levels of CES1A2 mRNA transcribed from the *CES1A2* gene might not be lower than those transcribed from the *CES1A1* variant. In the future, it will be interesting to determine the CES1A1 and CES1A2 mRNA levels as well as the CES1A protein levels and the subcellular localization in extrahepatic tissues, together with genotyping of the *CES1A1* variant and *CES1A2* or *CES1A3* gene.

It has been reported that a single nucleotide polymorphism (SNP) in the 5′-flanking region of the *CES1A2* gene, g.-861A > C, which was found in Japanese with 24.8% frequency, was associated with increased transcriptional activity and high responsiveness to imidapril [16]. In that report, the 5′-flanking regions of *CES1A2* and *CES1A3* were not distinguished. When we investigated our samples, out of 28 heterozygotes of *CES1A2/CES1A3*, the SNP was heterozygously detected in 13 participants and homozygously detected in one participant (data not shown) indicating that the SNP could be on both the *CES1A2* and *CES1A3* genes. To evaluate the clinical

Fig. 4

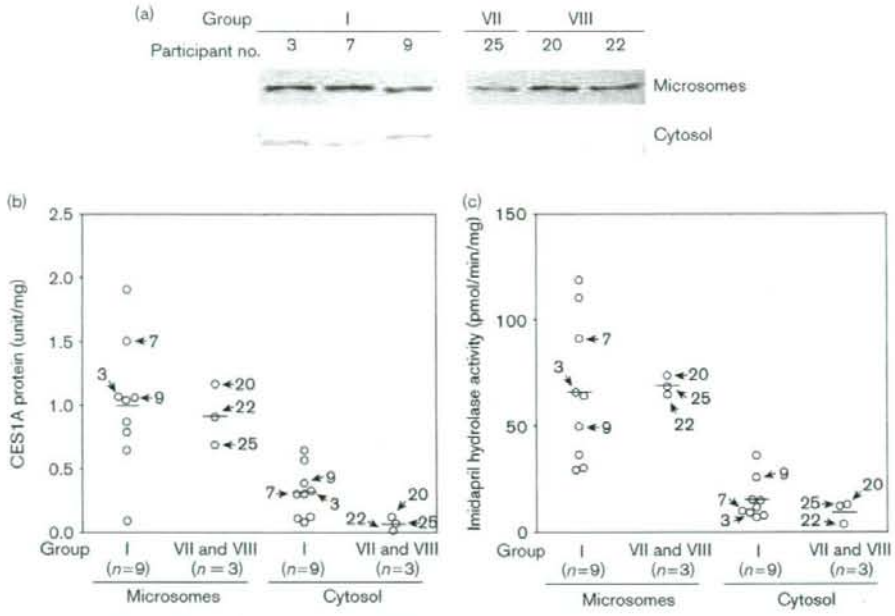

Carboxylesterase (CES) 1A protein levels and enzyme activity in human liver microsomes and cytosol. (a) Microsomes (5 μg) and cytosol (10 μg) fraction were separated by electrophoresis using 7.5% SDS-polyacrylamide gel. The CES1A protein was detected using rabbit anti-human *CES1A* antibody. Representative data for three out of nine samples in group I, one sample in group VII, and two samples in group VIII are shown. (b) The CES1A protein levels in group I ($n=9$) expressing only CES1A1 mRNA were compared with those in groups VII and VIII ($n=3$) expressing only CES1A2 mRNA. The average value of the CES1A protein levels in microsomes from group I was defined as 1 unit/mg. (c) Imidapril hydrolase activities in human liver microsomes and cytosol were determined by liquid chromatography-mass spectrometry (LC-MS/MS). The substrate concentration was 20 μmol/l. Horizontal bars show the average values in each group. The numbers with arrows show the sample numbers.

significance of the SNP, it should be determined whether the SNP was on the *CES1A2* or *CES1A3* gene because only the *CES1A2* gene encodes a functional enzyme.

Earlier studies reported that CES1A protein was mainly localized on the ER [17]. Our recent study, however, found that CES1A protein was also detected in cytosol fraction [18]. The CES1A protein purified from the human liver cytosol fraction had no signal peptide. The mechanisms regulating the subcellular localization of CES remain to be determined. Recently, Hosokawa [19] reported that no CES1A protein was detected in cytosol from human livers expressing only CES1A1 mRNA. In contrast to their report, in our western blot analysis a clear band was detected in cytosol from human livers expressing only CES1A1 mRNA (Figs 4a, b). We found that mature CES1A proteins derived from both CES1A1 and CES1A2 precursors were localized both in ER and cytosol, although the mature protein derived from the CES1A2 precursor was predominantly in the ER. The data of imidapril hydrolase activities in human liver microsomes and cytosol (Fig. 4c) supported the findings. Discordance between our and reported studies might be because of differences in the antibodies used and sensitivity or the conditions of the western blot analysis. These results presented here suggested that the differences in exon 1 encoding a signal peptide between CES1A1 and CES1A2 did not affect the subcellular localization.

As shown in Table 4 and Fig. 4, CES1A mRNA, protein levels, and enzyme activity in human livers were highly variable. The regulation mechanisms of CES1A expression are not fully understood, but it is conceivable that CES1A might be induced in response to xenobiotics from the environment or diet and endobiotics, and likely other drug metabolizing enzymes such as cytochrome P450 and uridine diphosphate. Genetic polymorphisms in the 5′-flanking region of *CES1A* genes would contribute to interindividual differences in CES1A expression. Further studies are required to understand the cause of the interindividual differences of the CES1A expression.

In conclusion, we found that the *CES1A2* gene is a variant of the *CES1A3* gene. The levels of CES1A2 mRNA transcribed from the *CES1A2* gene were substantially

lower than those transcribed from the *CES1A1* variant. The findings presented here significantly increase our understanding about the gene structure and expression properties of human CES1A.

Acknowledgement

The authors thank Brent Bell for reviewing the manuscript. None of the authors has any conflict of interest.

References

1 Imai T. Human carboxylesterase isozymes: catalytic properties and rational drug design. *Drug Metab Pharmacokinet* 2006; **21**:173–185.
2 Xu G, Zhang W, Ma MK, McLeod HL. Human carboxylesterase 2 is commonly expressed in tumor tissue and is correlated with activation of irinotecan. *Clin Cancer Res* 2002; **8**:2605–2611.
3 Sanghani SP, Quinney SK, Fredenburg TB, Davis WI, Murry DJ, Bosron WF. Hydrolysis of irinotecan and its oxidative metabolites, 7-ethyl-10-[4-N-(5-aminopentanoic acid)-1-piperidino] carbonyloxycamptothecin and 7-ethyl-10-[4-(1-piperidino)-1-amino]-carbonyloxycamptothecin, by human carboxylesterases CES1A1, CES2, and a newly expressed carboxylesterase isoenzyme, CES3. *Drug Metab Dispos* 2004; **32**:505–511.
4 Imai T, Taketani M, Shii M, Hosokawa M, Chiba K. Substrate specificity of carboxylesterase isoforms and their contribution to hydrolase activity in human liver and small intestine. *Drug Metab Dispos* 2006; **34**: 1734–1741.
5 Hosokawa M, Furihata T, Yaginuma Y, Yamamoto N, Koyano N, Fujii A, *et al.* Genomic structure and transcriptional regulation of the rat, mouse, and human carboxylesterase genes. *Drug Metab Rev* 2007; **39**:1–15.
6 Langmann T, Becker A, Aslanidis C, Notka F, Ullrich H, Schwer H, *et al.* Structural organization and characterization of the promoter region of a human carboxylesterase gene. *Biochim Biophys Acta* 1997; **1350**:65–74.
7 Tanimoto K, Kaneyasu M, Shimokuni T, Hiyama K, Nishiyama M. Human carboxylesterase 1A2 expressed from carboxylesterase 1A1 and 1A2 genes is a potent predictor of CPT-11 cytotoxicity *in vitro*. *Pharmacogenet Genomics* 2007; **17**:1–10.
8 Shibata F, Takagi Y, Kitajima M, Kubota Y, Omura T. Molecular cloning and characterization of a human carboxylesterase gene. *Genomics* 1993; **17**:76–82.
9 Yan B, Matoney L, Yang D. Human carboxylesterases in human placentae: enzymatic characterization, molecular cloning and evidence for the existence of multiple forms. *Placenta* 1999; **20**:599–607.
10 Fukami T, Nakajima M, Sakai H, McLead HL, Yokoi T. CYP2A7 polymorphic alleles confound the genotyping of CYP2A6*4A allele. *Pharmacogenomics J* 2006; **6**:401–412.
11 Nakajima M, Itoh M, Sakai H, Fukami T, Katoh M, Yamazaki H, *et al.* CYP2A13 expressed in human bladder metabolically activates 4-aminobiphenyl. *Int J Cancer* 2006; **119**:2520–2526.
12 Tsuchiya Y, Nakajima M, Kyo S, Kanaya T, Inoue M, Yokoi T. Human CYP1B1 is regulated by estradiol via estrogen receptor. *Cancer Res* 2004; **64**:3119–3125.
13 Tabata T, Katoh M, Tokudome S, Hosokawa M, Chiba K, Nakajima M, *et al.* Bioactivation of capecitabine in human liver: involvement of the cytosolic enzyme on 5′-deoxy-5-fluorocytidine formation. *Drug Metab Dispos* 2004; **32**:762–767.
14 Takahashi S, Katoh M, Saitoh T, Nakajima M, Yokoi T. Allosteric kinetics of human carboxylesterase 1: species differences and interindividual variability. *J Pharm Sci.* In press.
15 Hosokawa M, Furihata T, Yaginuma Y, Yamamoto N, Watanabe N, Tsukada E, *et al.* Structural organization and characterization of the regulatory element of the human carboxylesterase (CES1A1 and CES1A2) genes. *Drug Metab Pharmacokinet* 2008; **23**:73–84.
16 Geshi E, Kimura T, Yoshimura M, Suzuki H, Koba S, Sakai T, *et al.* A single nucleotide polymorphism in the carboxylesterase gene is associated with the responsiveness to imidapril medication and the promoter activity. *Hypertens Res* 2005; **28**:719–725.
17 Satoh T, Hosokawa M. The mammalian carboxylesterases: from molecules to functions. *Annu Rev Pharmacol Toxicol* 1998; **38**:257–288.
18 Tabata T, Katoh M, Tokudome S, Nakajima M, Yokoi T. Identification of the cytosolic carboxylesterase catalyzing the 5′-deoxy-5-fluorocytidine formation from capecitabine in human liver. *Drug Metab Dispos* 2004; **32**:1103–1110.
19 Hosokawa M. Structure and catalytic properties of carboxylesterase isozymes involved in metabolic activation of prodrugs. *Molecules* 2008; **13**:412–431.

0090-9556/09/3702-345–351$20.00
DRUG METABOLISM AND DISPOSITION

DMD 37:345–351, 2009

Vol. 37, No. 2
24521/3429942
Printed in U.S.A.

Metabolic Activation of Benzodiazepines by CYP3A4[S]

Katsuhiko Mizuno, Miki Katoh,[1] Hirotoshi Okumura, Nao Nakagawa, Toru Negishi, Takanori Hashizume, Miki Nakajima, and Tsuyoshi Yokoi

Drug Metabolism and Toxicology, Faculty of Pharmaceutical Sciences, Kanazawa University, Kanazawa, Japan (K.M., M.K., H.O., N.N., M.N., T.Y.); and Pharmacokinetics Research Laboratories, Dainippon Sumitomo Pharma Co., Ltd., Osaka, Japan (T.N., T.H.)

Received September 15, 2008; accepted November 10, 2008

ABSTRACT:

Cytochrome P450 3A4 is the predominant isoform in liver, and it metabolizes more than 50% of the clinical drugs commonly used. However, CYP3A4 is also responsible for metabolic activation of drugs, leading to liver injury. Benzodiazepines are widely used as hypnotics and sedatives for anxiety, but some of them induce liver injury in humans. To clarify whether benzodiazepines are metabolically activated, 14 benzodiazepines were investigated for their cytotoxic effects on HepG2 cells treated with recombinant CYP3A4. By exposure to 100 μM flunitrazepam, nimetazepam, or nitrazepam, the cell viability in the presence of CYP3A4 decreased more than 25% compared with that of the control. In contrast, in the case of other benzodiazepines, the changes in the cell viability between CYP3A4 and control Supersomes were less than 10%. These results suggested that nitrobenzodiazepines such as flunitrazepam, nimetazepam, and nitrazepam were metabolically activated by CYP3A4, which resulted in cytotoxicity. To identify the reactive metabolite, the glutathione adducts of flunitrazepam and nimetazepam were investigated by liquid chromatography-tandem mass spectrometry. The structural analysis for the glutathione adducts of flunitrazepam indicated that a nitrogen atom in the side chain of flunitrazepam was conjugated with the thiol of glutathione. Therefore, the presence of a nitro group in the side chain of benzodiazepines may play a crucial role in the metabolic activation by CYP3A4. The present study suggested that metabolic activation by CYP3A4 was one of the mechanisms of liver injury by nitrobenzodiazepines.

Drug-induced hepatotoxicity is one of the major causes of liver injury and is classified into intrinsic and idiosyncratic types. Intrinsic drug reactions can occur in a dose-dependent manner in any individual and are reproducible in preclinical studies. In contrast, idiosyncratic drug reactions do not occur in most patients at any dose, and they are often referred to as rare, with a typical incidence of from 1/100 to 1/100,000 (Uetrecht, 1999). Because idiosyncratic drug reactions are difficult to spot during drug development, some drugs launched on the market were later withdrawn because of idiosyncratic hepatotoxicity. Such drugs withdrawn for hepatotoxicity are known to produce reactive metabolites (Guengerich and MacDonald, 2007). The generation of reactive metabolites may relate to the formation of free radicals, oxidation of thiol, and covalent binding with endogenous macromolecules, resulting in the oxidation of cellular components or inhibition of normal cellular function (Guengerich and Liebler, 1985).

The generation of a reactive metabolite catalyzed by drug-metabolizing enzymes such as cytochrome P450 (P450) is defined as metabolic activation. P450 is the major drug-metabolizing enzyme that is highly expressed in human liver. CYP3A4 is the predominant isoform in liver (Shimada et al., 1994) and metabolizes more than 50% of the clinical drugs commonly used (Guengerich, 1995). However, CYP3A4 is also responsible for the formation of reactive metabolites of flutamide (Berson et al., 1993), trazodone (Kalgutkar et al., 2005), and troglitazone (Yamamoto et al., 2002). It is suggested that the reactive metabolites of flutamide, trazodone, and troglitazone cause the idiosyncratic hepatotoxicity in humans.

Prediction of the metabolic activation and the cytotoxicity of drug candidates is necessary in drug development. Human hepatocarcinoma HepG2 cells are commonly used for predicting hepatotoxicity in vitro. However, low expression levels of P450s in HepG2 cells may be responsible for the fact that 30% of the compounds were falsely classified as nontoxic (Rodriguez-Antona et al., 2002; Wilkening et al., 2003; Hewitt and Hewitt, 2004). In a recent study, a useful in vitro cell-based assay made by combining recombinant CYP3A4 with HepG2 cells was established (Vignati et al., 2005). It was demonstrated that hepatotoxicants whose reactive metabolites were generated by CYP3A4 exhibited cytotoxicity to the HepG2 cells. This assay system could be applied to screen for hepatotoxicity by drugs.

This study was supported by Young Scientists of the Ministry of Education, Culture, Sports, Science and Technology of Japan [Grant 19790120]; and Ministry of Health, Labor, and Welfare, Health and Labor Science Research [Grant H20-BI-001].

K.M. and M.K. contributed equally to this work.

[1] Current affiliation: Faculty of Pharmacy, Meijo University, Tempaku-ku, Nagoya, Japan.

Article, publication date, and citation information can be found at http://dmd.aspetjournals.org.

doi:10.1124/dmd.108.024521.

[S] The online version of this article (available at http://dmd.aspetjournals.org) contains supplemental material.

ABBREVIATIONS: P450, cytochrome P450; MTT, 3-(4,5-dimetylthiazol-2-yl)-2,5-diphenyl tetrazolium bromide; LC, liquid chromatography; MS/MS, tandem mass spectrometry; MS, mass spectrometry; LCMS-IT-TOF, liquid chromatography ion trap and time-of-flight mass spectrometry.

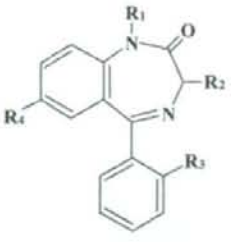

Benzodiazepine	R_1	R_2	R_3	R_4
Clonazepam	H	H	Cl	NO_2
Desmethyldiazepam	H	H	H	Cl
Diazepam	CH_3	H	H	Cl
Flunitrazepam	CH_3	H	F	NO_2
Flurazepam	$CH_2CH_2N(C_2H_5)$	H	F	Cl
Lorazepam	H	OH	Cl	Cl
Nimetazepam	CH_3	H	H	NO_2
Nitrazepam	H	H	H	NO_2
Norfludiazepam	H	H	F	Cl
Oxazepam	H	OH	H	Cl
Temazepam	CH_3	OH	H	Cl

FIG. 1. Chemical structures of the 14 benzodiazepines used in the present study.

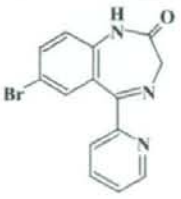

Bromazepam

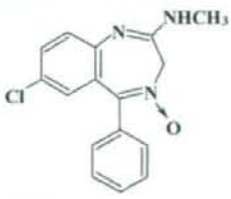

Chlordiazepoxide

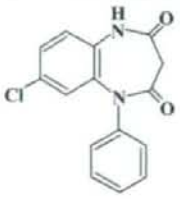

Clobazam

Benzodiazepines have been used extensively as hypnotics and sedatives for anxiety throughout the world. The mechanism of their efficacy is to amplify the action of γ-aminobutyric acid by acting as agonists at γ-aminobutyric acid receptors (Costa et al., 2002). Many benzodiazepines have been launched on the market and used in clinical practice. Two of the major benzodiazepines, flunitrazepam and nitrazepam, are widely used as hypnotic and anesthetic premedications in Europe and Japan. In 2001, it was announced by the Ministry of Health, Labor and Welfare of Japan that flunitrazepam induced hepatotoxicity. Chronic administration of antidepressant drugs including nitrazepam was reported to induce severe hepatic disorders (Seki et al., 2008). Clonazepam is one of the benzodiazepines used as an anxiolytic and anticonvulsant in clinical practice. Hepatic injury was reported to occur after treatment with clonazepam for 6 weeks in Ethiopia (Olsson and Zettergren, 1988).

The purpose of the present study was to clarify whether the metabolic activation of benzodiazepines by P450 occurs, leading to the hepatotoxicity. We investigated the cell viability in HepG2 cells in the presence or absence of CYP3A4 after exposure to 14 commercially available benzodiazepines (Fig. 1). There are many structural analogs of benzodiazepines, and the chemical structures and cytotoxicity in HepG2 cells were compared.

Materials and Methods

Materials. Clonazepam, clobazam, diazepam, lorazepam, nimetazepam, nitrazepam, and oxazepam were obtained from Wako Pure Chemicals (Osaka, Japan). Bromazepam, chlordiazepoxide, desmethyldiazepam, flunitrazepam, flurazepam, norfludiazepam, and temazepam were purchased from Sigma-Aldrich (St. Louis, MO). Human CYP2C9, 2C19, and 3A4 Supersomes (recombinant cDNA-expressed P450 enzymes prepared from a baculovirus insect cell system) and control Supersomes were purchased from BD Gentest (Woburn, MA). These microsomes coexpressed NADPH-cytochrome P450 reductase and cytochrome b_5. All other reagents used in this study were of the highest or analytical grade commercially available.

Cell Culture. Human hepatocarcinoma cell line HepG2 was obtained from Riken Gene Bank (Tsukuba, Japan). The cells were cultured in Dulbecco's modified Eagle's medium (Nissui Pharmaceutical, Tokyo, Japan) supplemented with 10% fetal bovine serum (Invitrogen, Melbourne, Australia) and 0.1 mM nonessential amino acids (Invitrogen) at 37°C in an atmosphere of 5% CO_2 and 95% air.

Cell Viability Assay. HepG2 cells were seeded at a density of 1×10^4 cells/well in 96-well plates with medium containing 3% fetal bovine serum, benzodiazepines, 8 nM human CYP2C9, CYP2C19, CYP3A4, or control Supersomes and 1 mM NADPH and then incubated at 37°C for 24 h. In the preliminary study, we investigated the cell viability in HepG2 cells with various P450 concentrations and incubation time. The 8 nM P450 and 24-h incubation were enough to detect cytotoxicity in this assay system. The final concentration of organic solvent (dimethyl sulfoxide) in medium was less than 0.2%. Cell viability after a 24-h incubation was evaluated by the intracellular ATP concentration using a CellTiter-Glo Luminescent Cell Viability Assay (ATP assay; Promega, Madison, WI) and 3-(4,5-dimetylthiazol-2-yl)-2,5-diphenyl tetrazolium bromide (MTT) activities using a CellTiter-Blue Cell Viability Assay (MTT assay; Promega). According to the protocols of the manufacturer, the luminescence of the generated oxyluciferin was measured in the ATP assay and the fluorescence of the generated resorufin was detected fluorometrically (excitation: 338 nm, emission: 458 nm) in the MTT assay by using a 1420 ARVO MX luminometer (PerkinElmer Wallac, Turku, Finland).

Caspase Assay. HepG2 cells were seeded under the same conditions and incubated at 37°C for 24 h. After incubation, the caspase 3/7 activity was measured using a Caspase-Glo 3/7 Assay (Promega) according to the protocol of the manufacturer. The luminescence of the generated aminoluciferin was measured using a 1420 ARVO MX luminometer.

Detection of Glutathione Adducts. A typical reaction mixture (final volume of 0.25 ml) contained 50 nM human CYP3A4 Supersomes, 100 mM potassium phosphate buffer (pH 7.4), an NADPH-generating system consisting of 0.775 mM nicotinamide adenine dinucleotide phosphate (oxidized form), 0.165 mM glucose 6-phosphate, 0.165 mM $MgCl_2$, 0.2 unit/ml glucose-6-phosphate dehydrogenase, 10 mM glutathione (reduced form), and 100 μM benzodiazepines (flunitrazepam, nimetazepam, nitrazepam, bromazepam, or temazepam). The final concentration of dimethyl sulfoxide in the reaction mixture was less than 1%. Incubation was performed at 37°C for 60 min and terminated by adding 0.75 ml of ice-cold methanol. After centrifugation at 15,000*g*, the supernatant was subjected to liquid chromatography-tandem mass spectrometry (LC-MS/MS) (API 4000; Applied Biosystems, Foster City, CA). An LC-10 liquid chromatograph (Shimadzu, Kyoto, Japan) was used with an Inertsil ODS-3 analytical column (2.1 × 100 mm, 3 μm; GL Science, Tokyo, Japan). The column temperature was 40°C. The mobile phase was 10 mM ammonium acetate buffer (pH 4.0) (A) and acetonitrile (B). The conditions for

elution were as follows: 5 to 90% B (0–6 min), 90% B (6–11 min), 90 to 5% B (11–11.01 min), and 5% B (11.01–15 min). Linear gradients were used for all solvent changes. The flow rate was 0.2 ml/min. The liquid chromatograph was connected to an API 4000 mass spectrometer operated in the negative electrospray ionization mode. The turbo gas was maintained at 450°C. Air was used as the nebulizing and turbo gas at 60 psi. Nitrogen was used as the curtain gas at 20 psi. The collision energy was −50 V. The *m/z* 300 to 850 was scanned at the precursor ion (*m/z* 272; major mass spectrum fragment of glutathione).

Identification of Glutathione Adducts. Liquid chromatography ion trap and time-of-flight mass spectrometry (LCMS-IT-TOF) (Shimadzu) was used to identify the structures of the glutathione adducts of the nitrobenzodiazepines. The incubation mixture was the same as that described above except for CYP3A4 Supersomes (100 nM). Flunitrazepam and nimetazepam were used as test compounds. After centrifugation at 15,000*g* for 5 min, the supernatant was subjected to LCMS-IT-TOF using an Inertsil ODS-3 analytical column (2.1 × 100 mm, 3 μm). The LC conditions were the same as described earlier. The turbo gas was maintained at 450°C. Air was used as the nebulizing and turbo gas at 60 psi. Nitrogen was used as the curtain gas at 20 psi. The collision energy was 50 V. Structure analysis of the glutathione adducts of flunitrazepam and nimetazepam was performed by scanning at the product ion (*m/z* 621 and *m/z* 603, respectively) in the positive electrospray ionization mode.

Statistics. Data are expressed as mean ± S.D. ($n = 3$). Two groups were compared with a two-tailed Student's t test. $P < 0.05$ was considered statistically significant.

Results

Cell Viability of HepG2 Cells Treated with CYP3A4 and Benzodiazepines. HepG2 cells were incubated for 24 h with the 14 benzodiazepines at 50, 100, 200, and 400 μM in the presence of CYP3A4 or control Supersomes and then the cell viability was measured by the ATP and MTT assays. With exposure to 100 μM flunitrazepam, nimetazepam, and nitrazepam, cell viability in the presence of CYP3A4 Supersomes decreased more than 25% than with control Supersomes (Fig. 2). Although clonazepam could be dissolved up to 100 μM in the reaction mixtures, the viability of HepG2 cells treated with CYP3A4 Supersomes and 100 μM clonazepam exhibited 57 and 35% decreases in the ATP and MTT assays, respectively, compared with viability with control Supersomes (Supplemental Fig. 2). Flunitrazepam, nimetazepam, nitrazepam, and clonazepam are nitrobenzodiazepines that have a nitro group at the 7-position (Fig. 1). In contrast, for the other 10 benzodiazepines (bromazepam, chlordiazepoxide, clobazam, desmethyldiazepam, diazepam, flurazepam, lorazepam, norfludiazepam, oxazepam, and temazepam) at 100 μM, the changes in cell viability between CYP3A4 and control Supersomes were less than 10% and much smaller than those for the nitrobenzodiazepines (Fig. 2 and Supplemental Fig. 1). Moreover, 25% effective concentrations (EC_{25}) of nitrobenzodiazepines were less than 100 μM, and EC_{25} values of all other benzodiazepines were more than 300 μM in the ATP assay (Supplemental Table 1). Desmethyldiazepam, diazepam, flurazepam, lorazepam, norfludiazepam, and oxazepam exhibited concentration-dependent cytotoxicity in HepG2 cells incubated both with and without CYP3A4 (Fig. 2 and Supplemental Fig. 1).

Cell Viability on HepG2 Cells Treated with CYP2Cs and Nitrobenzodiazepines. It has been reported that CYP2C9 and CYP2C19 are involved in the metabolism of flunitrazepam (Hesse et al., 2001; Kilicarslan et al., 2001). Therefore, we investigated whether CYP2C9 and CYP2C19 affect the cytotoxicity caused by nitrobenzodiazepines in HepG2 cells. As shown in Fig. 3, the differences in the cell viability between CYP2Cs and control Supersomes when exposed to 100 μM nitrobenzodiazepines were less than 10%.

Caspase 3/7 Activity in HepG2 Cells Treated with CYP3A4 and Nitrobenzodiazepines. As a key factor of apoptosis, the caspase 3/7 activity was measured in HepG2 cells treated with CYP3A4 and the nitrobenzodiazepines for 24 h. Flunitrazepam, nimetazepam, and nitrazepam significantly increased the caspase 3/7 activities in HepG2 cells in the presence of CYP3A4 Supersomes (Fig. 4, A–C). In contrast, bromazepam as the negative control had no effects on the caspase 3/7 activities both with and without CYP3A4 (Fig. 4D).

Detection of Glutathione Adducts of Benzodiazepines. The glutathione adducts of benzodiazepines were investigated by the negative ion mode of LC-MS/MS. The nitrobenzodiazepines (flunitrazepam, nimetazepam, and nitrazepam) and the negative controls (bromazepam and temazepam) were measured. As shown in Fig. 5, the glutathione adducts of flunitrazepam and nimetazepam were detected in the presence of CYP3A4 Supersomes by precursor ion scans at *m/z* 619 and *m/z* 601 ($[M - H]^-$), respectively. In contrast, there were no adducts of flunitrazepam and nimetazepam when they were used in the control Supersomes (data not shown). In nitrazepam, bromazepam, and temazepam, glutathione adducts were not detected in the presence and absence of CYP3A4.

Identification of Glutathione Adducts of Flunitrazepam and Nimetazepam. The structures of the glutathione adducts of flunitrazepam and nimetazepam were estimated by the positive ion mode of LCMS-IT-TOF. For of the glutathione adduct of flunitrazepam, the product ion mass spectrum of *m/z* 621 ($[M + H]^+$) gave fragment ions at *m/z* 284.1, *m/z* 348.1, and *m/z* 492.1. The molecule weight of the $[M + H]^+$ fragment ion (*m/z* 492.1) meant that it was produced by the molecule weight of the compound (491) and that of a hydrogen ion (H^+; 1). The possible structure of the glutathione adduct of flunitrazepam is shown in Fig. 6. A reactive metabolite of flunitrazepam, in which the nitro group might be metabolized into the amino group, was conjugated to the 7-substituent group by glutathione.

On the other hand, the $[M + H]^+$ ion of the glutathione adduct of nimetazepam (*m/z* 603) gave fragment ions at *m/z* 266.4 and *m/z* 474.2 (Supplemental Fig. 3). The fragment ions at *m/z* 266.4 and *m/z* 474.2 were $[M + H - 337]^+$ and $[M + H - 129]^+$, respectively, corresponding to the fragment ions at *m/z* 284.1 and *m/z* 492.1 obtained from the glutathione adduct of flunitrazepam (*m/z* 621).

Discussion

In the present study, 14 benzodiazepine analogs were investigated for cytotoxic effects resulting from metabolic activation by CYP3A4. The major metabolic pathways of diazepam are 3-hydroxylayion by CYP3A4 and *N*-desmethylation by CYP2C9 (Schwartz et al., 1965; Ono et al., 1996). Thus, desmethyldiazepam, temazepam, and oxazepam are metabolites of diazepam (Fig. 1). In addition, norfludiazepam and nitrazepam would be the metabolites of flurazepam and nimetazepam, respectively.

The cytotoxicity of flunitrazepam, nimetazepam, nitrazepam, and clonazepam was observed in the presence of CYP3A4 Supersomes in HepG2 cells (Fig. 2 and Supplemental Fig. 1), suggesting that these three drugs are metabolically activated by CYP3A4. Flunitrazepam, nimetazepam, nitrazepam, and clonazepam are classified as nitrobenzodiazepines that have a nitro group in the side chain. In contrast, the other 10 benzodiazepines exhibited less cytotoxicity than the nitrobenzodiazepines (Fig. 2 and Supplemental Fig. 1; Supplemental Table 1). In the present study, we first clarified that the presence of a nitro group in the side chain of benzodiazepines may play a crucial rule in the metabolic activation by CYP3A4. To prevent the cytotoxicity by reactive metabolites in the medium, the effects of 200 μM or 1 mM glutathione (reduced form) were measured in this cell viability assay as a preliminary experiment. The glutathione recovered 10% of cell viability in HepG2 cells treated with CYP3A4 and 100 μM flunitraz-

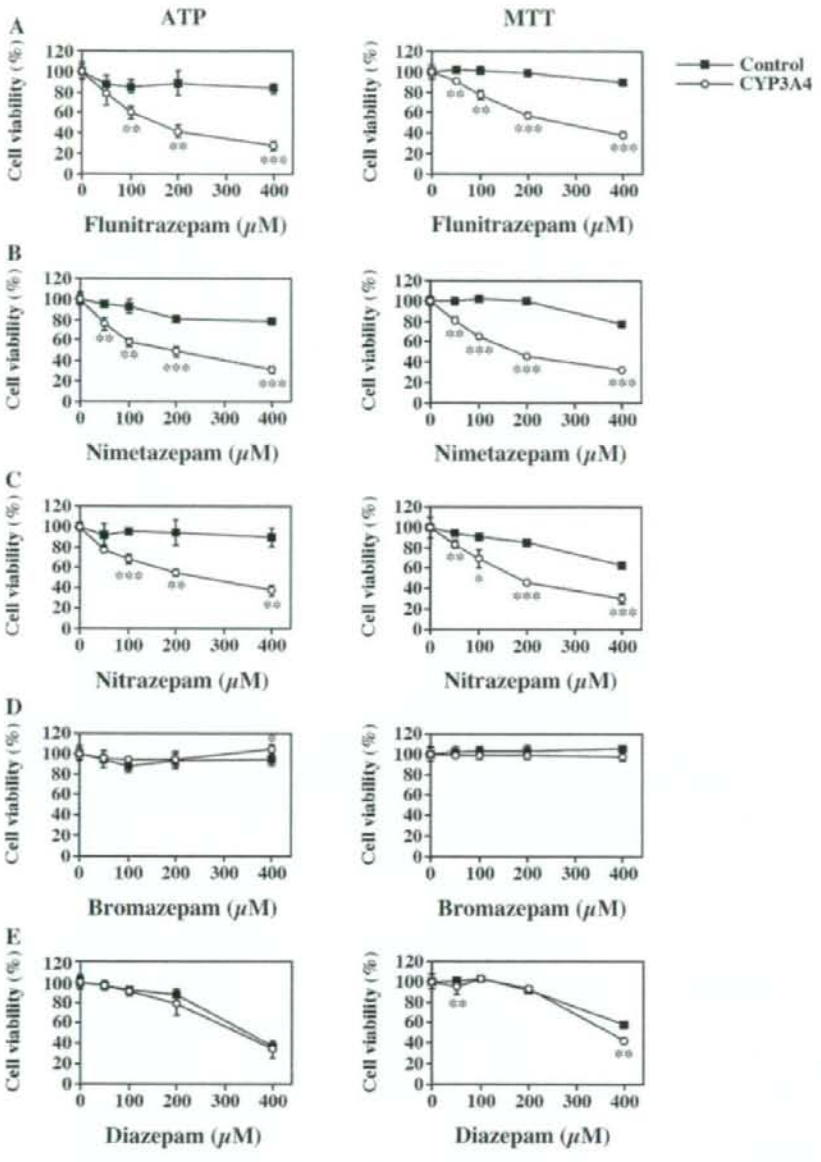

FIG. 2. Cytotoxicity of the benzodiazepines incubated with CYP3A4 on HepG2 cells. HepG2 cells seeded with the benzodiazepines and CYP3A4 or control Supersomes in 96-well plates were incubated at 37°C for 24 h. Cell viability was measured by ATP assay (left) and MTT assay (right) as described under *Materials and Methods*. The test compounds were flunitrazepam (A), nimetazepam (B), nitrazepam (C), bromazepam (D), and diazepam (E). Data represent the mean ± S.D. of three independent experiments. *, $P < 0.05$; **, $P < 0.01$; ***, $P < 0.001$, compared with the control Supersomes.

epam (data not shown). This finding suggested that the reactive metabolites of nitrobenzodiazepines may bind to glutathione. However, glutathione did not completely protect against the cytotoxicity; thus, there may be another cytotoxic effect that could not be detoxified by glutathione trapping.

In humans, the major metabolites of flunitrazepam are *N*-desmethylflunitrazepam in plasma and 3-hydroxyflunitrazepam and 7-aminoflunitrazepam in urine (Fukazawa et al., 1978). CYP3A4 is the major P450 involved in flunitrazepam 3-hydroxylation and *N*-desmethylation, but CYP2C9 and CYP2C19 also catalyze the *N*-desmethylation of flunitrazepam (Hesse et al., 2001; Kilicarslan et al., 2001). The reductive metabolite of flunitrazepam, 7-aminoflunitrazepam, is catalyzed by NADPH-cytochrome P450 reductase in HepG2 cells (Peng et al., 2004). Nimetazepam is metabolized to *N*-desmethylnimetazepam and 3-hydroxylnimetazepam (Dainippon Sumitomo Pharma, unpublished data). Nitrazepam is metabolized to 7-aminonitrazepam and 3-hydroxynitrazepam (Rieder, 1965). Although which P450 isoform mediates nimetazepam and nitrazepam metabolism has not been revealed, nimetazepam and nitrazepam may be metabolized by CYP2C9, CYP2C19, and CYP3A4. In our study, when HepG2 cells were exposed to 100 μM nitrobenzodiazepines, the differences in the cell viability between CYP2Cs and control Supersomes were less than 10% (Fig. 3), indicating that the contribution of CYP2Cs to the cytotoxicity of nitrobenzodiazepines was much lower than that of

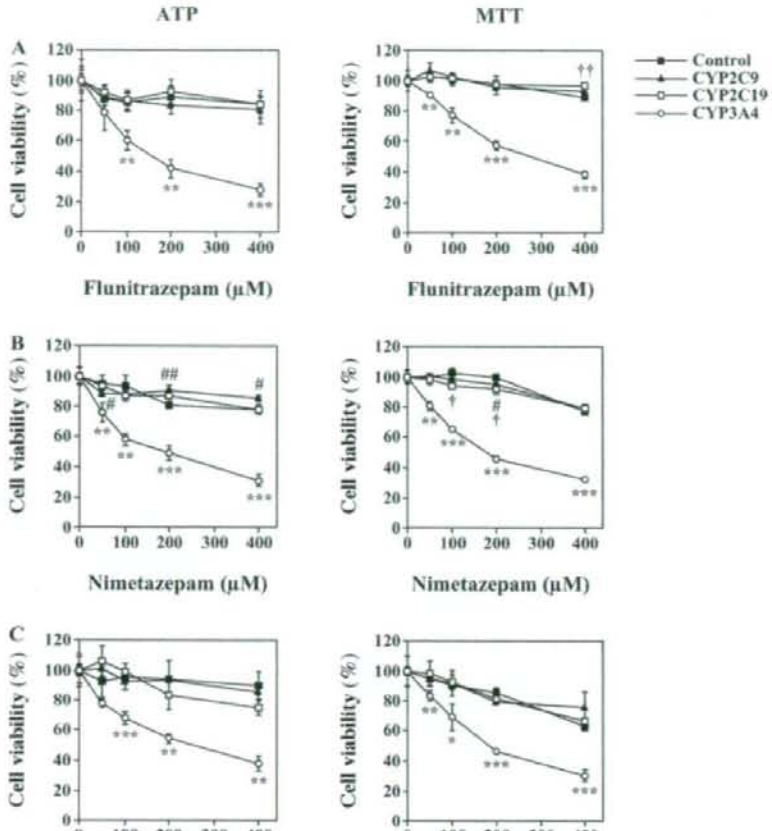

FIG. 3. Cytotoxicity of the benzodiazepines incubated with CYP2Cs in HepG2 cells. HepG2 cells seeded with the benzodiazepines and CYP2C9, CYP2C19, or control Supersomes in 96-well plates were incubated at 37°C for 24 h. Cell viability was measured by ATP assay (left) and MTT assay (right) as described under *Materials and Methods*. The test compounds were flunitrazepam (A), nimetazepam (B), and nitrazepam (C). Data for CYP3A4 and control Supersomes were redrawn from Fig. 2. Data represent the mean ± S.D. of three independent experiments. #, $P < 0.05$; ##, $P < 0.01$ (CYP2C9); †, $P < 0.05$; ††, $P < 0.01$ (CYP2C19); *, $P < 0.05$; **, $P < 0.01$; ***, $P < 0.001$ (CYP3A4), compared with the control Supersomes.

CYP3A4. Therefore, the metabolic activations of the nitrobenzodiazepines were CYP3A4-specific reactions.

Caspase 3 and 7 are classified as effector caspases. Active effector caspases mediate the cleavage of an overlapping set of protein substrates, resulting in the morphological features of apoptosis and the demise of the cell (Nuñez et al., 1998). Flunitrazepam, nimetazepam, and nitrazepam significantly increased the caspase 3/7 activities in HepG2 cells in the presence of CYP3A4 Supersomes (Fig. 4). Therefore, apoptosis after caspase 3 and 7 activation is one of the cytotoxic pathways of the reactive metabolites of flunitrazepam, nimetazepam, and nitrazepam.

The maximum plasma concentrations of nitrobenzodiazepines after a single administration in humans have been reported as follows: 0.04 μM after an oral dose of 2 mg of flunitrazepam (Fukazawa et al., 1978), 0.05 μM after an oral dose of 5 mg of nimetazepam (Dainippon Sumitomo Pharma, unpublished data), 0.3 μM after an oral dose of 10 mg of nitrazepam (Rieder, 1973), and 0.05 μM after an oral dose of 2 mg of clonazepam (Cavedal et al., 2007). Flunitrazepam was reported to induce hepatotoxicity by the Ministry of Health, Labor and Welfare of Japan, and nitrazepam and clonazepam were reported to cause drug-induced liver injury (Olsson and Zettergren, 1988; Seki et al., 2008). Although it is very difficult to extrapolate from an in vitro study to in vivo in humans, we may pay attention to the metabolic activation of nitrobenzodiazepines by CYP3A4.

The metabolism of a nontoxic drug to reactive metabolites is thought to initiate a variety of adverse reactions (Park, 1986; Parke, 1987). Glutathione is an important intracellular peptide that can detoxify reactive metabolites by conjugation (Lu, 1999). Previous studies reported that reactive metabolites of flutamide (Kang et al., 2007), trazodone (Kalgutkar et al., 2005), and troglitazone (Kassahun et al., 2001) formed by CYP3A4 were detoxified by glutathione conjugations. As shown in Fig. 5, glutathione adducts of flunitrazepam and nimetazepam were detected by LC-MS/MS, suggesting the production of reactive metabolites of flunitrazepam and nimetazepam catalyzed by CYP3A4. In the present study, the structure of the glutathione adduct of flunitrazepam was estimated by LCMS-IT-TOF as shown in Fig. 6. It seemed that a nitrogen atom in the side chain of flunitrazepam was conjugated with the thiol of glutathione. The structure of the glutathione adduct of nimetazepam may be similar to that of flunitrazepam because the fragment ions, $[M + H - 337]^+$ and $[M + H - 129]^+$, corresponded to those of flunitrazepam (Supplemental Fig. 3). The glutathione adducts of nitrazepam could not be detected either with or without CYP3A4 in our detection system. However, the cytotoxicity of nitrazepam to HepG2 cells treated with CYP3A4

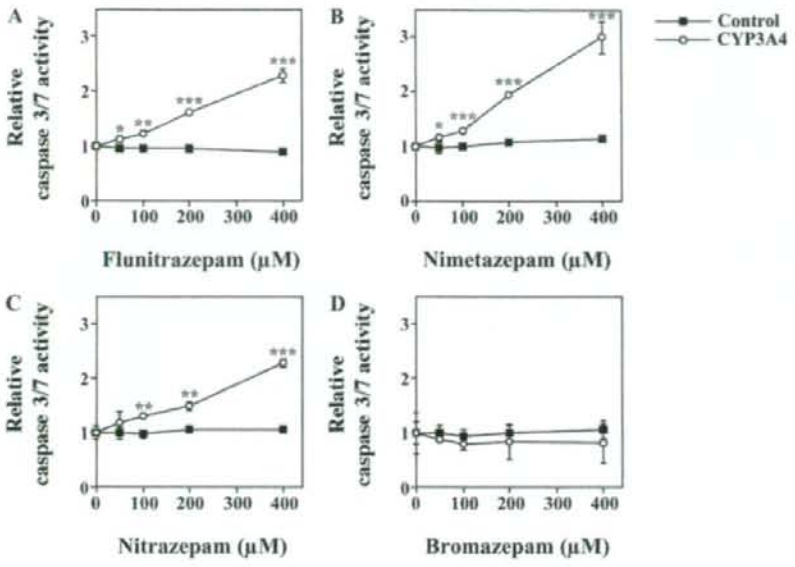

FIG. 4. Caspase 3/7 activity in HepG2 cells treated with CYP3A4 and the nitrobenzodiazepines. HepG2 cells in 96-well plates were incubated with benzodiazepines and CYP3A4 or control Supersomes at 37°C for 24 h. Caspase 3/7 activity was measured as described under *Materials and Methods*. The test compounds were flunitrazepam (A), nimetazepam (B), nitrazepam (C), and bromazepam (D). Data represent the mean ± S.D. of three independent experiments. *, $P < 0.05$; **, $P < 0.01$; ***, $P < 0.001$, compared with the control Supersomes.

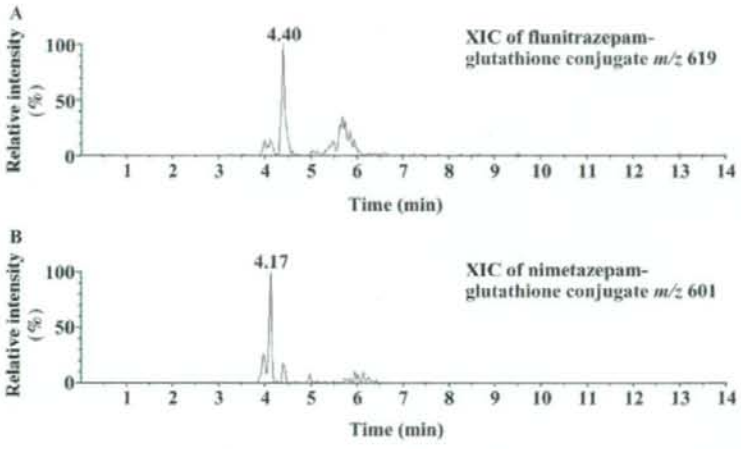

FIG. 5. Exacted ion chromatograms (XIC) of the glutathione adducts of benzodiazepines. The chromatograms were scanned with the precursor ion fragment, *m/z* 272, derived from glutathione using LC-MS/MS. A, flunitrazepam at *m/z* 619 ($[M - H]^-$); B, nimetazepam at *m/z* 601 ($[M - H]^-$).

Supersomes (Fig. 2) suggested that metabolic activation might occur. One of the reasons for this discrepancy may be the sensitivity of the detection.

Nitroaromatic drugs such as flutamide, nimesulide, and tolcapone have been associated with idiosyncratic liver injury (Boelsterli et al., 2006). In the reductive pathways from nitro to the fully reduced amine catalyzed by P450 and/or reductase, several reactive metabolites including nitroso and *N*-hydroxylamine derivatives could be produced. Such reactive metabolites seem to bind covalently to nucleophilic targets of proteins and nucleic acids, leading to the cytotoxic effects (Biaglow et al., 1986; Rickert, 1987; Kedderis and Miwa, 1988; Kedderis et al., 1989). On the other hand, arylamines are metabolically activated by P450-mediated *N*-hydroxylation. Electrophilic *N*-hydroxylamine reacts with intracellular molecules, which induce various types of toxicity including hepatotoxicity (Kato and Yamazoe, 1994). Flutamide induced severe hepatic dysfunction. Ohbuchi et al. (2008) suggested that CYP3A4 catalyzed the *N*-oxidation of the amino metabolite of flutamide, which had hepatotoxic effects. Although the bioactivation pathways of nitrobenzodiazepines still remain unclear, they may undergo metabolic activation similar to that of other drugs. Further study is needed to clarify the mechanism of metabolic activation concerning nitrobenzodiazepines.

In conclusion, we revealed that nitrobenzodiazepines, such as flunitrazepam, nimetazepam, and nitrazepam, were metabolically activated by CYP3A4, resulting in cytotoxicity in HepG2 cells. The CYP3A4 metabolites of flunitrazepam and nimetazepam were conjugated with glutathione at a nitrogen atom in the side chain. This finding suggested that metabolic activation by CYP3A4 may be one of the mechanisms in liver injury. Moreover, we established a simple assay system in which the cytotoxicity in HepG2 cells incubated with recombinant P450s and the drug was observed with high sensitivity. This assay system was useful for detecting metabolic activation by P450s and would be beneficial for predicting drug-induced cytotoxicity in preclinical drug development.

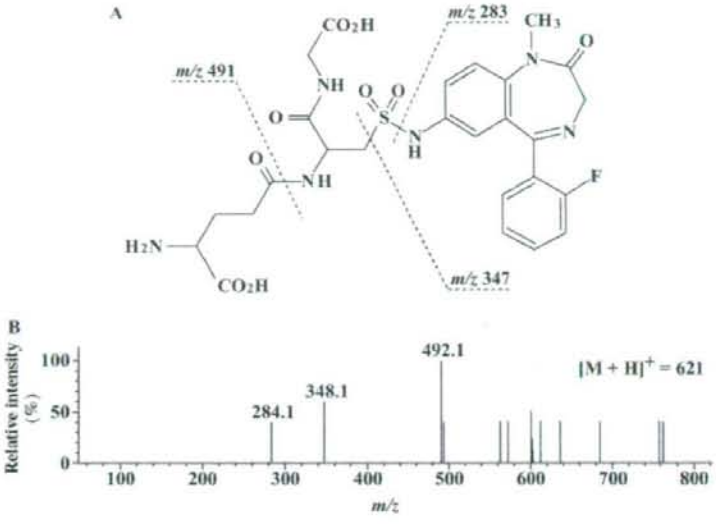

FIG. 6. A, predicted structure of the glutathione adduct of flunitrazepam. B, MS/MS spectra of the product ion obtained by collision-induced dissociation of the glutathione adduct of flunitrazepam at *m/z* 621 ([M + H]$^+$). These spectra were scanned using LCMS-IT-TOF.

Acknowledgments. We acknowledge Brent Bell for reviewing the article.

References

Berson A, Wolf C, Chachaty C, Fisch C, Fau D, Eugene D, Loeper J, Gauthier JC, Beaune P, and Pompon D (1993) Metabolic activation of the nitroaromatic antiandrogen flutamide by rat and human cytochromes P-450, including forms belonging to the 3A and 1A subfamilies. *J Pharmacol Exp Ther* **265**:366–372.

Biaglow JE, Varnes ME, Roizen-Towle L, Clark EP, Epp ER, Astor MB, and Hall EJ (1986) Biochemistry of reduction of nitro heterocycles. *Biochem Pharmacol* **35**:77–90.

Boelsterli UA, Ho HK, Zhou S, and Leow KY (2006) Bioactivation and hepatotoxicity of nitroaromatic drugs. *Curr Drug Metab* **7**:715–727.

Cavedal LE, Mendes FD, Domingues CC, Patni AK, Monif T, Reyar S, Pereira Ados S, Mendes GD, and De Nucci G (2007) Clonazepam quantification in human plasma by high-performance liquid chromatography coupled with electrospray tandem mass spectrometry in a bioequivalence study. *J Mass Spectrom* **42**:81–88.

Costa E, Auta J, Grayson DR, Matsumoto K, Pappas GD, Zhang X, and Guidotti A (2002) $GABA_A$ receptors and benzodiazepines: a role for dendritic resident subunit mRNAs. *Neuropharmacology* **43**:925–937.

Fukazawa H, Ichishita H, Honda M, and Shimazu H (1978) Pharmacokinetics studies of flunitrazepam in healthy male Japanese subjects. *Jpn J Clin Pharmacol Ther* **9**:251–265.

Guengerich FP (1995) Human cytochrome P-450 enzymes, in *Cytochrome P-450* (Ortiz de Montellano PR eds) pp. 473–535, Premium, New York.

Guengerich FP and Liebler DC (1985) Enzymatic activation of chemicals to toxic metabolites. *Crit Rev Toxicol* **14**:259–307.

Guengerich FP and MacDonald JS (2007) Applying mechanisms of chemical toxicity to predict drug safety. *Chem Res Toxicol* **20**:344–369.

Hesse LM, Venkatakrishnan K, von Moltke LL, Shader RI, and Greenblatt DJ (2001) CYP3A4 is the major CYP isoform mediating the in vitro hydroxylation and demethylation of flunitrazepam. *Drug Metab Dispos* **29**:133–140.

Hewitt NJ and Hewitt P (2004) Phase I and II enzyme characterization of two sources of HepG2 cell lines. *Xenobiotica* **34**:243–256.

Kalgutkar AS, Henne KR, Lame ME, Vaz AD, Collin C, Soglia JR, Zhao SX, and Hop CE (2005) Metabolic activation of the nontricyclic antidepressant trazodone to electrophilic quinone-imine and epoxide intermediates in human liver microsomes and recombinant P4503A4. *Chem Biol Interact* **155**:10–20.

Kang P, Dalvie D, Smith E, Zhou S, and Deese A (2007) Identification of a novel glutathione conjugate of flutamide in incubations with human liver microsomes. *Drug Metab Dispos* **35**:1081–1088.

Kassahun K, Pearson PG, Tang W, McIntosh I, Leung K, Elmore C, Dean D, Wang R, Doss G, and Baillie TA (2001) Studies on the metabolism of troglitazone to reactive intermediates in vitro and in vivo. Evidence for novel biotransformation pathways involving quinone methide formation and thiazolidinedione ring scission. *Chem Res Toxicol* **14**:62–70.

Kato R and Yamazoe Y (1994) Metabolic activation of *N*-hydroxylated metabolites of carcinogenic and mutagenic arylamines and arylamides by esterification. *Drug Metab Rev* **26**:413–429.

Kedderis GL, Argenbright LS, and Miwa GT (1989) Covalent interaction of 5-nitroimidazoles with DNA and protein in vitro: mechanism of reductive activation. *Chem Res Toxicol* **2**:146–149.

Kedderis GL and Miwa GT (1988) The metabolic activation of nitroheterocyclic therapeutic agents. *Drug Metab Rev* **19**:33–62.

Kilicarslan T, Haining RL, Rettie AE, Busto U, Tyndale RF, and Sellers EM (2001) Flunitrazepam metabolism by cytochrome P450s 2C19 and 3A4. *Drug Metab Dispos* **29**:460–465.

Lu SC (1999) Regulation of hepatic glutathione synthesis: current concepts and controversies. *FASEB J* **13**:1169–1183.

Nuñez G, Benedict MA, Hu Y, and Inohara N (1998) Caspases: the proteases of the apoptotic pathway. *Oncogene* **17**:3237–3245.

Ohbuchi M, Miyata M, Nagai D, Shimada M, Yoshinari K, and Yamazoe Y (2008) Role of enzymatic *N*-hydroxylation and reduction in flutamide metabolite-induced liver toxicity. *Drug Metab Dispos* **37**:97–105.

Olsson R and Zettergren L (1988) Anticonvulsant-induced liver damage. *Am J Gastroenterol* **83**:576–577.

Ono S, Hatanaka T, Miyazawa S, Tsutsui M, Aoyama T, Gonzalez FJ, and Satoh T (1996) Human liver microsomal diazepam metabolism using cDNA-expressed cytochrome P450s: role of CYP2B6, 2C19 and 3A subfamily. *Xenobiotica* **26**:1155–1166.

Park BK (1986) Metabolic basis of adverse drug reaction. *J R Coll Phys Lond* **20**:195–200.

Parke DV (1987) Activation mechanisms to chemical toxicity. *Arch Toxicol* **60**:5–15.

Peng FC, Chaing HH, Tang SH, Chen PC, and Lu SC (2004) NADPH-cytochrome P-450 reductase is involved in flunitrazepam reductive metabolism in HepG2 and Hep3B cells. *J Toxicol Environ Health A* **67**:109–124.

Rickert DE (1987) Metabolism of nitroaromatic compounds. *Drug Metab Rev* **18**:23–53.

Rieder J (1965) Methods for estimating 1,3-dihydro-7-nitro-5-phenyl-2*H*-1,4-benzodiazepin-2-one and its principal metabolites in biological samples and results of research on the pharmacokinetics and metabolism of this compound in humans and rats. *Arzneimittel-Forschung* **15**:1134–1148.

Rieder J (1973) Plasma levels and derived pharmacokinetic characteristics of unchanged nitrazepam in man. *Arzneimittel-Forschung* **23**:212–218.

Rodriguez-Antona C, Donato MT, Boobis A, Edwards RJ, Watts PS, Castell JV, and Gómez-Lechón MJ (2002) Cytochrome P450 expression in human hepatocytes and hepatoma cell lines: molecular mechanisms that determine lower expression in cultured cells. *Xenobiotica* **32**:505–520.

Schwartz MA, Koechlin BA, Postma E, Palmer S, and Krol G (1965) Metabolism of diazepam in rat, dog, and man. *J Pharmacol Exp Ther* **149**:423–435.

Seki E, Taniguchi H, Nagano R, Sakitani Y, Serizawa T, Ito Y, Mine N, Mizuno H, Mitsuno Y, and Nakata R (2008) Case report: severe hepatic disorder induced by chronic administration of antidepressants drugs. *552nd Meeting for the Japanese Society of Internal Medicine Kanto Division*; 2008 Mar 8; Tokyo, Japan. 31 p, The Japanese Society of Internal Medicine, Tokyo.

Shimada T, Yamazaki H, Mimura M, Inui Y, and Guengerich FP (1994) Interindividual variations in human liver cytochrome P-450 enzymes involved in the oxidation of drugs, carcinogens and toxic chemicals: studies with liver microsomes of 30 Japanese and 30 Caucasians. *J Pharmacol Exp Ther* **270**:414–423.

Uetrecht JP (1999) New concepts in immunology relevant to idiosyncratic drug reactions: the "danger hypothesis" and innate immune system. *Chem Res Toxicol* **12**:387–395.

Vignati L, Turlizzi E, Monaci S, Grossi P, Kanter R, and Monshouwer M (2005) An in vitro approach to detect metabolite toxicity due to CYP3A4-dependent bioactivation of xenobiotics. *Toxicology* **216**:154–167.

Wilkening S, Stahl F, and Bader A (2003) Comparison of primary human hepatocytes and hepatoma cell line HepG2 with regard to their biotransformation properties. *Drug Metab Dispos* **31**:1035–1042.

Yamamoto Y, Yamazaki H, Ikeda T, Watanabe T, Iwabuchi H, Nakajima M, and Yokoi T (2002) Formation of a novel quinone epoxide metabolite of troglitazone with cytotoxicity to HepG2 cells. *Drug Metab Dispos* **30**:155–160.

Address correspondence to: Dr. Tsuyoshi Yokoi, Drug Metabolism and Toxicology, Faculty of Pharmaceutical Sciences, Kanazawa University, Kakuma-machi, Kanazawa 920-1192, Japan. E-mail: tyokoi@kenroku.kanazawa-u.ac.jp

DMD Fast Forward. Published on February 18, 2009 as doi:10.1124/dmd.108.024331

DMD #24331

Different Inhibitory Effects in Rat and Human Carboxylesterases

Shiori Takahashi, Miki Katoh, Takashi Saitoh, Miki Nakajima, and Tsuyoshi Yokoi

Drug Metabolism and Toxicology, Faculty of Pharmaceutical Sciences, Kanazawa University, Kanazawa 920-1192, Japan.

Running title: Species differences in CES inhibition.

To whom all correspondence should be sent:

Tsuyoshi Yokoi, Ph.D.

Drug Metabolism and Toxicology

Faculty of Pharmaceutical Sciences

Kanazawa University

Kakuma-machi

Kanazawa 920-1192, Japan

Tel / Fax: +81-76-234-4407

E-mail: tyokoi@kenroku.kanazawa-u.ac.jp

This manuscript consists of 23 pages of text, 2 tables, 3 figures, and 28 references.

Abstract: 248 words

Introduction: 395 words

Discussion: 1146 words

[1]Abbreviations used are: CES, carboxylesterase; NDGA, nordihydroguaiaretic acid; CPT-11, irinotecan hydrochloride; DMSO, dimethyl sulfoxide; HLM, human liver microsomes; HLC, human liver cytosol; HJM, human jejunum microsomes; HJC, human jejunum cytosol; RLM, rat liver microsomes; RLC, rat liver cytosol; RJM, rat jejunum microsomes; RJC, rat jejunum cytosol; BNPP, bis (*p*-nitrophenyl) phosphate; HPLC, high-performance liquid chromatography; *Ki*, inhibition constant

ABSTRACT

In vitro inhibition studies on drug metabolizing enzyme activity are useful for understanding drug-drug interactions and for drug development. However, the profile of the inhibitory effects of carboxylesterase (CES) activity has not been fully investigated concerning species and tissue differences. In the present study, we measured the inhibitory effects of 15 drugs and one compound on CES activity using liver and jejunum microsomes and cytosol in human and rat. In addition, the inhibition constant (Ki values) and patterns were determined for the compounds exhibiting strong inhibition. Hydrolysis of imidapril and irinotecan hydrochloride (CPT-11) is mainly catalyzed by CES1 and CES2, respectively. In the inhibition study, imidaprilat formation from imidapril in human liver was strongly inhibited by nordihydroguaiaretic acid (NDGA) and procainamide. The inhibition profile and pattern were similar in human liver and rat liver. The compounds showing potent inhibition were similar between liver and jejunum. The Ki value of NDGA (Ki = 13.3 ± 1.5 μM) in human liver microsomes was 30-fold higher than that in rat liver microsomes (Ki = 0.4 ± 0.0 μM). On the other hand, SN-38 formation from CPT-11 was not inhibited except by carvedilol, manidipine, and physostigmine. The Ki value of physostigmine (Ki = 0.3 ± 0.0 μM) in human jejunum cytosol was 10-fold lower than that in rat jejunum cytosol (Ki = 3.1 ± 0.4 μM) and was similar to manidipine. The present study clarified the species differences in CES inhibition. These results are useful for the development of prodrugs.

INTRODUCTION

Carboxylesterase (CES) belongs to the α/ß-hydrolase fold family and plays an important role in the hydrolysis of many esterified drugs such as anticancer and antihypertension drugs. There are species differences in CES isoforms between human and rat. In human, two major CES isoforms designated CES1 and CES2 have been characterized and CES3 has been recently found in liver at considerably lower expression levels than the other CES isoforms (Sanghani et al., 2004). The mRNA expression levels of human CES1 are higher in liver than those in small intestine (Satoh et al., 2002), whereas human CES2 is abundant in small intestine (Schwer et al., 1997). On the other hand, in rat, there are several isoforms in CES1 and CES2 families. In the CES1 family, ES-10 (hydrolase A), ES-4 (hydrolase B/C), and ES-3 are mainly expressed in liver and the mRNA expression levels of ES-10 are the highest of the three isoforms (Linke et al., 2005). ES-2 has been identified as CES (Murakami et al., 1993) and can be hardly detected in liver (Sanghani et al., 2002). Three rat CES2 genes D50580, AB010635, and AY034877 have been found in various tissues such as liver, small intestine, stomach, and kidney (Sanghani et al., 2002).

The co-administration of drugs can affect their efficacy. Alterations in drug metabolism such as oxidation, reduction, and hydrolysis are often important causes of drug interactions. In particular, since inhibition of drug-metabolizing enzymes is recognized as a prevalent factor, it is necessary to understand and clarify the inhibitory effects. The inhibitory effects of some compounds on CES activity have been previously reported on isomalathion (Buratti and Testai, 2005) and trifluoromethylketone-containing compounds (Wadkins et al., 2007). An anticancer drug, tamoxifen, has been found to be an inhibitor of human CES1 (Fleming et al., 2005) and rat ES-10 (Mésange et al., 2002).

However, species differences in the inhibitory effects on CES activity have never been investigated comprehensively. In pre-clinical development of prodrugs catalyzed by esterases, information on differences in the inhibitory properties between rat and human is useful. In the present study, imidapril, an inhibitor of angiotensin-converting enzyme and irinotecan hydrochloride (CPT-11) were used as typical substrates for CES1 and CES2, respectively (Takai et al., 1997; Sanghani et al., 2004; Humerickhouse et al., 2000). We investigated the species differences in the inhibitory effects of 15 drugs and one compound for two representative CES activities.

Materials and Methods

Materials. Imidapril hydrochloride and imidaprilat were kindly supplied by Mitsubishi Tanabe Pharma Corporation (Osaka, Japan). Delapril was kindly provided by Takeda Pharmaceutical Company (Osaka, Japan). Capecitabine was purchased from The United States Pharmacopeial Convention (Rockville, MD). Carvedilol was obtained from LKT Laboratories (St. Paul, MN). CPT-11, SN-38, docetaxel trihydrate, temocapril hydrochloride, and temocaprilat were purchased from Toronto Research Chemicals (North York, On, Canada). Acemetacin, dexamethasone, nordihydroguaiaretic acid (NDGA), procainamide hydrochloride, and proglumide were purchased from Sigma-Aldrich (St. Louis, MO). Camptothecin, ciprofloxacin hydrochloride monohydrate, manidipine, nifedipine, and physostigmine sulfate were obtained from Wako Pure Chemicals (Osaka, Japan). Pooled human liver microsomes (HLM) and cytosol (HLC) were purchased from BD Gentest (Woburn, MA). Pooled human jejunum microsomes (HJM) and cytosol (HJC) were obtained from Tissue Transformation

Technologies (Edison, NJ). All other chemicals and solvents were of analytical or the highest grade commercially available.

Preparation of Microsomes and Cytosol from Rat Liver or Jejunum. Male Wistar rats, 7 weeks old, were obtained from Japan SLC (Shizuoka, Japan). Pooled microsomes and cytosol from 5 rat livers (RLM and RLC) and jejunums (RJM and RJC) were prepared according to the method of Emoto et al. (2001).

Imidaprilat Formation. Imidaprilat formation from imidapril was determined according to the method of Takahashi et al. (2008) with slight modifications. A typical incubation mixture (200 μl of total volume) contained the enzyme source, 100 mM tris(hydroxymethyl)aminomethane-HCl buffer (pH 7.4), and inhibitors. After a 2-min preincubation at 37°C, the reaction was initiated by the addition of imidapril and then the mixture was incubated at 37°C for 30 min except for RLM and RLC (10 min). The reaction was terminated by adding 100 μl of ice-cold acetonitrile. After centrifugation at 9,000*g* for 5 min, 10 μl of the supernatant were subjected to liquid chromatography-tandem mass spectrometry system. The formed imidaprilat was quantified by the LC-MS/MS peak area of an authentic standard. The linearity of the standard curve of imidaprilat was confirmed ($r = 0.99$) and the imidaprilat in the incubation mixture was determined within the range. In the preliminary study, bis (*p*-nitrophenyl) phosphate (BNPP), a CES specific inhibitor, (300 μM) inhibited the imidaprilat formation potently with all enzyme sources at 150 μM imidapril.

SN-38 Formation. SN-38 formation from CPT-11 was determined according to the method of Tabata et al. (2004) with slight modifications. A typical incubation mixture (200 μl of total volume) contained the enzyme source, 100 mM potassium phosphate buffer (pH 7.4), and inhibitors. CPT-11 was dissolved in dimethyl sulfoxide (DMSO).

The final concentration of DMSO in the reaction mixture was < 1.0%. After a 2-min preincubation at 37°C, the reaction was initiated by the addition of CPT-11 and then the mixture was incubated at 37°C for 3 min except for RJM and RJC (2 min). The reaction was terminated by adding 200 μl of ice-cold acetonitrile and 10 μl of 1 M HCl were then added. Camptothecin (20 pmol) was added as an internal standard. After centrifugation at 6,500*g* for 5 min, 50 μl of the supernatant were subjected to high-performance liquid chromatography (HPLC) equipped with an Inertsil ODS-3 analytical column (4.6 x 250 mm; GL Science). The eluent was fluorometrically monitored at an excitation of 380 nm and emission of 556 nm with a noise-base clean Uni-3 (Union, Gunma, Japan). The column temperature was 35°C and the flow rate was 0.8 ml/min. The mobile phase consisted of 30% acetonitrile and 70% of 10 mM KH_2PO_4 containing 30 mM 1-heptanesulfonic acid sodium salt. The retention times of SN-38 and camptothecin were 13.3 and 16.3 min, respectively. The formed SN-38 was quantified by the HPLC peak height of an authentic standard. The linearity of the standard curve of SN-38 was confirmed ($r = 0.99$) and the SN-38 in the incubation mixture was determined within the range. In the preliminary study, BNPP (10 μM) inhibited the SN-38 formation potently with all enzyme sources at 5 μM CPT-11.

Inhibition Analysis of CES Activities. The inhibitory effects on the imidaprilat and SN-38 formation were investigated using 15 drugs and one compound. Acemetacin, capecitabine, carvedilol, CPT-11, dexamethasone, docetaxel, manidipine, NDGA, nifedipine, temocapril, and temocaprilat were dissolved in DMSO. Ciprofloxacin, delapril, imidapril, physostigmine, procainamide, and proglumide were dissolved in distilled water. Capecitabine, delapril, and temocapril are CES substrates, whereas the other drugs and one compound are not. These compounds were added to the incubation

mixtures described above to investigate their inhibitory effects on the imidaprilat and SN-38 formations. The final concentration of DMSO in the incubation mixture was < 1% except for manidipine (2%) in the imidaprilat formation. All data were analyzed using the average of duplicate determinations.

For screening of the inhibitory effects, the imidaprilat formation at 150 μM imidapril was examined in the presence of 15 drugs and one compound (300 μM) except manidipine (50 μM). The SN-38 formation at 5 μM CPT-11 was determined in the presence of 15 drugs and one compound (10 μM).

For determination of the *Ki* (inhibition constant) values, the concentrations of imidapril ranged from 100 to 500 μM for HLM and HLC, from 25 to 150 μM for RLM, from 15 to 90 μM for RLC, from 20 to 80 μM for RJM, and from 25 to 100 μM for RJC, respectively. The concentrations of the inhibitors ranged as follows: carvedilol, 1-6 μM for RLM, 1-6 μM for RLC, 4-24 μM for RJM, and 5-30 μM for RJC; NDGA, 10-40 μM for HLM, 2-7 μM for HLC, 0.2-2 μM for RLM, 0.2-1.5 μM for RLC, 3-15 μM for RJM, and 2-12 μM for RJC; procainamide, 25-150 μM for HLM and 25-100 μM for HLC. The protein concentrations of HLM, HLC, RLM, RLC, RJM, and RJC were 0.2, 1.0, 0.01, 0.05, 0.2, and 0.5 mg/ml, respectively. In the preliminary study, the rate of imidaprilat formation was linear with respect to the all protein concentrations and incubation time.

For determination of the *Ki* values, the concentrations of CPT-11 ranged from 2.5 to 15 μM for all enzyme sources and the inhibitors ranged as follows: carvedilol, 2-8 μM for HLM and 1-12 μM for HLC; manidipine, 0.1-0.5 μM for HJC, 0.5-5 μM for RJM, and 0.5-4 μM for RJC; physostigmine, 0.1-0.6 μM for HLM, 0.2-5 μM for HLC, 1-6 μM for HJM, 0.2-1 μM for HJC, 1-8 μM for RJM, and 2-10 μM for RJC. The protein concentrations of microsomes and cytosol were 0.2 and 1.0 mg/ml except for RJM and

RJC (0.1 and 0.5 mg/ml), respectively. In the preliminary study, the rate of SN-38 formation was linear with respect to the all protein concentrations and incubation time. The *Ki* values and inhibition types were determined by fitting the kinetic data to a competitive, noncompetitive, uncompetitive, or mixed inhibition model by nonlinear regression analysis using GraphPad Prism 5 (GraphPad Software, San Diego, CA).

Results

Inhibitory Effects of 15 Drugs and One Compound on Imidaprilat Formation. The inhibitory effects on the imidaprilat formation were investigated using 15 drugs and one compound (Fig. 1). The imidaprilat formation in both HLM and HLC were moderately inhibited by acemetacin, carvedilol (only HLC), nifedipine, and procainamide (20-50% of control), and strongly inhibited by NDGA (< 20% of control). On the other hand, all compounds except ciprofloxacin, dexamethasone (only RLC), and proglumide inhibited the imidaprilat formation by more than 50% in both RLM and RLC. In particular, delapril, temocapril, and temocaprilat, which are structurally similar to imidapril, showed stronger inhibitions in RLM and RLC than in HLM and HLC. The compounds exhibiting strong inhibition in RJM and RJC were similar to those in RLM and RLC. Imidaprilat formation in HJM and HJC was not detected at 200 μM imidapril, therefore inhibition studies were not performed.

Inhibitory Effects of 15 Drugs and One Compound on SN-38 Formation. Fifteen drugs and one compound were screened for the inhibitory effects on the SN-38 formation (Fig. 2). Screening of the inhibitory effects in HJM and HJC were performed only for 6 drugs and one compound because the lots of HJM and HJC available were limited. In both HLM and HLC, carvedilol, physostigmine, and manidipine (only HLC) inhibited the

SN-38 formation moderately (20-50% of control). In both RLM and RLC, SN-38 formation was not inhibited except by manidipine and NDGA, exhibiting weak inhibition (50-70% of control) only in RLC. These formations in both RJM and RJC were inhibited moderately by manidipine and physostigmine. The SN-38 formation in HJC was inhibited moderately by carvedilol (20-50% of control) and inhibited strongly by manidipine and physostigmine, whereas this formation in HJM was inhibited strongly only by physostigmine.

Inhibition Constant and Inhibitory Patterns of Imidaprilat Formation. The *K*i values and inhibition patterns of the compounds showing strong inhibition for the imidaprilat formation were determined (Table 1) and representative Lineweaver-Burk plots are shown in Fig. 3 (A, B, and C). The *K*i value of NDGA in HLM was 30-fold higher than that in RLM, suggesting species differences. The *K*i value of NDGA in RLM was also much lower than that in RJM. Similarly, NDGA in RLC showed a lower *K*i value than that in RJC. The inhibitory potency of procainamide in HLM was similar to that in HLC. The *K*i value of carvedilol in RJM was approximately 5-fold higher than that in RLM. Compared with microsomes and cytosol from rat liver or jejunum, the *K*i values of carvedilol were approximately 2-fold different.

Inhibition Constant and Inhibitory Patterns of SN-38 Formation. The *K*i values and inhibition patterns for the SN-38 formation were determined as shown in Table 2 and representative Lineweaver-Burk plots are shown in Fig. 3 (D, E, and F). The *K*i values in RLM and RLC were not determined because the activity was not inhibited potently by any drugs or compound. The *K*i value of carvedilol in HLM was lower than that in HLC. The *K*i value of physostigmine in HJM was similar to RJM. On the other hand, the *K*i value of physostigmine in HJC was 10-fold lower than that in RJC or HJM. The